

# Gravastar energy conditions revisited

Dubravko Horvat and Saša Ilić

Department of Physics, Faculty of Electrical Engineering and Computing, University of Zagreb, Unska 3, HR-10 000 Zagreb, Croatia

E-mail: [dubravko.horvat@fer.hr](mailto:dubravko.horvat@fer.hr), [sasa.ilijic@fer.hr](mailto:sasa.ilijic@fer.hr)

**Abstract.** We consider the gravastar model where the vacuum phase transition between the de Sitter interior and the Schwarzschild or Schwarzschild–de Sitter exterior geometries takes place at a single spherical  $\delta$ -shell. We derive sharp analytic bounds on the surface compactness ( $2m/r$ ) that follow from the requirement that the dominant energy condition (DEC) holds at the shell. In the case of Schwarzschild exterior, the highest surface compactness is achieved with the stiff shell in the limit of vanishing (dark) energy density in the interior. In the case of Schwarzschild–de Sitter exterior, in addition to the gravastar configurations with the shell under surface pressure, gravastar configurations with vanishing shell pressure (dust shells), as well as configurations with the shell under surface tension, are allowed by the DEC. Respective bounds on the surface compactness are derived for all cases. We also consider the speed of sound on the shell as derived from the requirement that the shell is stable against the radial perturbations. The causality requirement (sound speed not exceeding that of light) further restricts the space of allowed gravastar configurations.

PACS numbers: 04.40.Dg

## 1. Introduction

The gravastar model has been proposed by Mazur and Mottola (MM) as a possible end point of the gravitational collapse of a massive body [1, 2]. As opposed to the classical scenario of the gravitational collapse into a Schwarzschild black hole, the gravastar concept avoids the formation of the black hole horizon. Technically, the gravastar is a global, static, spherically symmetric solution to the Einstein equations. In the interior there is a segment of the de Sitter geometry which is matched to the exterior Schwarzschild geometry by means of a spherical shell of matter. In the original MM model the quantum phase transition takes place within the boundary layer/shell, but the full quantum treatment is immediately replaced by the mean field approximation in which (classical) Einstein equations are valid. The de Sitter geometry in the interior of the gravastar implies constant positive (dark) energy density  $\rho$  accompanied by the isotropic negative pressure  $p = -\rho$ . Such energy-momentum content of the spacetime is equivalent to introducing the positive cosmological constant  $\lambda = 8\pi\rho$  into the Einstein equations, and can be understood as the gravitational vacuum, or gravitational

condensate, which motivated the coining of the term gravastar (*gravitational vacuum star*). In this original model of MM, the phase transition layer consists of two spherical  $\delta$ -shells with vanishing surface energy density but with non-vanishing surface pressure, between which there is a thin layer of stiff matter ( $\rho = p > 0$ ). The transition layer is positioned arbitrarily close to where the horizon of the Schwarzschild geometry is expected to form. In this way the gravastar model allows for arbitrarily high gravitational surface red-shifts and is, for an external observer, indistinguishable from being a true black hole.

A simplified gravastar model was constructed by Visser and Wiltshire [3] in order to study the stability properties. The phase transition layer was replaced by a single spherical  $\delta$ -shell. The issue of stability could not be fully settled because the equation of state for the shell is not available. However, it was shown that physically reasonable equations of state could lead to gravastar configurations that are stable against radial perturbations. This simplified gravastar model also motivated a number of authors to consider different vacuum geometries in the interior and the exterior. This includes the models with anti-de Sitter interior and the Schwarzschild–de Sitter exterior geometries and also the Reissner–Nordström geometries [4], the Born–Infeld phantom gravastar [5], and the non-linear electrodynamics gravastar [6]. A different development of the gravastar idea went in the direction of constructing models with continuous profiles for the energy density and the anisotropic pressures [7, 8]. In these models the energy momentum tensor in the centre of the spherical structure satisfies  $\rho = -p$  and through the layer of anisotropic principal pressures (crust) smoothly joins with the exterior vacuum spacetime. Gravastars with shells of finite thickness but without  $\delta$ -shells at the boundaries with the vacuum regions have been considered in Ref. [9] and it has been pointed out that quasi-normal modes of oscillations might be a possible way of distinguishing gravastars from black holes. An account of the observational constraints placed on the gravastar model has been given in Ref. [10]. The gravastar models are also closely related to a broader subject of dark energy stars, see eg. Ref. [11]. In fact, the ideas of astrophysical bodies with the de Sitter core representing the gravitationally collapsed matter at extremely high density can be traced back to the work of Sakharov [12] and Gliner [13] and have been further investigated by Dymnikova in a series of papers starting with [14], see eg. Refs [15, 16] and references therein.

Given that the physical mechanism behind the proposed vacuum phase transition within the gravastar shell is essentially unknown, the energy conditions of GR [17] provide the most widely accepted framework of model-of-matter independent constraints one can impose on the ‘exotic matter’ comprising the shell. It is therefore important to fully investigate the constraints on the gravastar model that are imposed by the energy conditions. In this work we will consider the  $\delta$ -shell gravastar model of Ref [3] and we will derive the sharp analytic bounds on the surface compactness that follow from the requirement that the dominant energy condition (DEC) is satisfied at the shell. The DEC will include the weak (WEC) and the null energy conditions (NEC), but not the strong energy condition (SEC). Since the SEC is violated from the outset by the dark

energy in the interior of the gravastar, it does not appear natural to require that it holds throughout the phase transition layer.

In Sec. 2 we review the  $\delta$ -shell gravastar model and we introduce the configuration variables that we use through the rest of the paper. In Sec. 3 we discuss the energy conditions of GR imposed on the energy-momentum tensor of the gravastar shell and in Sec. 4 we carry out the detailed analysis of the gravastar configurations allowed by the DEC. In Sec. 5 we discuss the properties of the equation of state as derived from the assumed stability of the gravastar with respect to radial perturbations. Conclusions are given in Sec. 6.

## 2. The gravastar model

The line element for the interior and the exterior geometries can be written using the geometrized units  $G = 1 = c$  and the coordinates  $x^\alpha = (t, r, \vartheta, \varphi)$  in the form

$$ds^2 = g_{\alpha\beta} dx^\alpha dx^\beta = -k(1 - \mu(r)) dt^2 + \frac{1}{1 - \mu(r)} dr^2 + r^2 d\Omega^2 \quad (1)$$

where  $d\Omega^2 = d\vartheta^2 + \sin^2 \vartheta d\varphi^2$  is the metric on the unit 2-sphere,  $k > 0$  is the time coordinate scaling constant, and  $\mu(r)$  is the *compactness function* related to the quasi-local mass function  $m(r)$  by

$$\mu(r) = \frac{2m(r)}{r} = \frac{2}{r} \int_0^r 4\pi \bar{r}^2 \rho(\bar{r}) d\bar{r}, \quad (2)$$

where  $\rho(r)$  is the energy density. In general, to avoid the formation of the event horizon within the spherical body the compactness must be less than unity.

In the interior of the gravastar shell we have the segment of the de Sitter geometry with the constant energy density  $\rho_{\text{int}} = \lambda_{\text{int}}/8\pi \geq 0$  and the compactness is given by

$$\mu_{\text{int}}(r) = \frac{8\pi}{3} \rho_{\text{int}} r^2 = \frac{\lambda_{\text{int}}}{3} r^2, \quad r < a. \quad (3)$$

At  $r = (3/\lambda_{\text{int}})^{1/2}$  the interior compactness reaches unity which corresponds to the position of the de Sitter (cosmological) horizon. Therefore the surface of the gravastar must be located at the radius  $r = a < (3/\lambda_{\text{int}})^{1/2}$ .

In the exterior we have the Schwarzschild–de Sitter geometry with the constant energy density  $\rho_{\text{ext}} = \lambda_{\text{ext}}/8\pi \geq 0$  and mass parameter  $M > 0$ . The exterior compactness is given by

$$\mu_{\text{ext}}(r) = \frac{2M}{r} + \frac{8\pi}{3} \rho_{\text{ext}} r^2 = \frac{2M}{r} + \frac{\lambda_{\text{ext}}}{3} r^2, \quad r > a. \quad (4)$$

With  $\lambda_{\text{ext}} = 0$ ,  $M > 0$ , this is clearly the Schwarzschild geometry, while with  $\lambda_{\text{ext}} > 0$ ,  $M = 0$ , this is the de Sitter geometry. In the general case we are considering,  $\lambda_{\text{ext}} > 0$ ,  $M > 0$ , the gravastar surface must be located in the region where  $\mu_{\text{ext}} < 1$ . For this region to exist the condition  $9M^2\lambda_{\text{ext}} < 1$  must hold, whereupon the radial coordinates of the two horizons of the Schwarzschild–de Sitter geometry which bound the region are given by the roots of  $\mu_{\text{ext}}(r) = 1$  (a cubic). Thus, if the gravastar surface is located

at  $r = a$  such that  $\mu_{\text{int}}(a) < 1$  and  $\mu_{\text{ext}}(a) < 1$ , no horizon forms within the gravastar geometry up to the outer horizon of the Schwarzschild–de Sitter geometry.

Since the original motivation behind the MM gravastar model was to construct a highly compact object that could represent a gravitationally collapsed body of positive gravitational mass, one expects the (dark) energy density inside the gravastar to be greater than that of the surrounding space, i.e.  $\rho_{\text{int}} \geq \rho_{\text{ext}}$ , or equivalently  $\lambda_{\text{int}} \geq \lambda_{\text{ext}}$ . We refer to the above as the “gravastar requirement”. Note also that the constants  $\lambda_{\text{int}}$  and  $\lambda_{\text{ext}}$  are introduced for notational convenience; however,  $\lambda_{\text{ext}}$  can be viewed as the cosmological constant  $\Lambda = \lambda_{\text{ext}}$  present in the Einstein equations provided that in the exterior of the gravastar shell we set  $\rho_{\text{ext}} \rightarrow \rho'_{\text{ext}} = 0$  and in the interior we set  $\rho_{\text{int}} \rightarrow \rho'_{\text{int}} = (\lambda_{\text{int}} - \lambda_{\text{ext}})/8\pi$ . Thus, in the picture with the cosmological constant, demanding that the energy density in the interior of the gravastar shell is non-negative,  $\rho'_{\text{int}} \geq 0$ , is equivalent to our “gravastar requirement”. Therefore, although it *is* technically possible to construct the gravastar-like solutions to the Einstein equations with  $\rho_{\text{int}} < \rho_{\text{ext}}$  and  $M > 0$ , we will not consider them in this analysis.

Through the rest of the paper we will describe the gravastar configurations in terms of the configuration variables defined as follows:

$$\begin{aligned} x &= \mu_{\text{int}}(a) = \lambda_{\text{int}} a^2/3, \\ y &= \mu_{\text{ext}}(a) = 2M/a + \lambda_{\text{ext}} a^2/3 = 2M/a + z, \\ z &= \lambda_{\text{ext}} a^2/3. \end{aligned} \tag{5}$$

$x$  and  $y$  are the values of the compactness on the interior and the exterior side of the shell, while  $z$  is the contribution to the compactness at the exterior side of the shell due to the energy density in the exterior.

For the gravastar geometry we require

$$0 \leq z \leq x \leq y < 1. \tag{6}$$

$z$  and  $x$  are non-negative since the energy densities in the interior and in the exterior are non-negative by assumption. The condition  $z \leq x$  reflects the above mentioned ‘gravastar requirement’. The condition  $y \geq z$  ensures that the mass of the gravastar,  $M$ , is non-negative, while  $y \geq x$ , as will be shown in Sec. 3, ensures that the energy density of the gravastar shell is non-negative.

The gravastar shell is a timelike hypersurface of constant radius  $r = a$  along which the interior and the exterior geometries are joined. The Israel’s thin shell formalism [18] (for textbook coverage see eg. [19, 20]) allows one to assign the energy-momentum distribution to the hypersurface, as required to make the resulting spacetime a solution of Einstein equations. The first junction condition requires that the induced metric on the hypersurface be the same for the metrics on both sides of the hypersurface. Parametrizing the hypersurface with the coordinates  $y^a = (t, \vartheta, \varphi)$ , the hypersurface metric tensor  $h_{ab}$  as induced from the metric (1) is given by  $h_{ab} = g_{\alpha\beta} e_a^\alpha e_b^\beta$ , where  $e_a^\alpha = \partial x^\alpha / \partial y^a$ . The hypersurface line element is given by

$$ds^2 = h_{ab} dy^a dy^b = -k(1 - \mu(a)) dt^2 + a^2 d\Omega^2. \tag{7}$$

Therefore, for the first junction condition to hold we must have  $k_{\text{int}}(1 - \mu_{\text{int}}(a)) = k_{\text{ext}}(1 - \mu_{\text{ext}}(a))$ . This is accomplished by setting  $k_{\text{ext}} = 1$  for compatibility with the usual form of the exterior Schwarzschild metric in case  $\lambda_{\text{ext}} = 0$ , and setting  $k_{\text{int}} = (1 - y)/(1 - x)$  to appropriately rescale the time coordinate in the interior. The second junction condition requires that for the smooth joining of the metrics on the two sides of the hypersurface the extrinsic curvature on the hypersurface,  $K_{ab} = n_{\alpha;\beta} e_a^\alpha e_b^\beta$ , be the same on both sides of the hypersurface. The nonvanishing components of the extrinsic curvature for the hypersurface of radius  $r = a$  embedded in the metric of the form (1) are

$$K_t^t = -\frac{\mu'(a)}{2\sqrt{1-\mu(a)}} \quad \text{and} \quad K_\vartheta^\vartheta = K_\varphi^\varphi = \frac{1}{a}\sqrt{1-\mu(a)}. \quad (8)$$

In the gravastar the second junction condition is not satisfied. The joining of the metrics is not smooth, but is still possible if one allows for the energy-momentum distribution on the hypersurface. The standard expression for the shell energy-momentum tensor on a timelike hypersurface is

$$S_b^a = -\frac{1}{8\pi} ([K_b^a] - [K]\delta_b^a), \quad (9)$$

where the brackets denote the discontinuity of the quantity over the hypersurface and  $K = K_a^a$ . Using the compactness functions for the exterior and interior metric given by (3) and (4) and the notation (5), the surface energy density can be written

$$\sigma = -S_t^t = -\frac{1}{4\pi a} [\sqrt{1-\mu(a)}] = \frac{1}{4\pi a} (\sqrt{1-x} - \sqrt{1-y}), \quad (10)$$

and the isotropic surface tension can be written

$$\begin{aligned} \theta = -S_\vartheta^\vartheta = -S_\varphi^\varphi &= -\frac{1}{8\pi a} \left[ \frac{1 - \mu(a) - r\mu'(a)/2}{\sqrt{1-\mu(a)}} \right] \\ &= \frac{1}{8\pi a} \left( \frac{1-2x}{\sqrt{1-x}} - \frac{1-\frac{1}{2}y-\frac{3}{2}z}{\sqrt{1-y}} \right). \end{aligned} \quad (11)$$

Note that by definition the surface tension has the opposite sign of the surface pressure, i.e.,  $\theta > 0$  indicates that the surface (shell) is ‘under tension’, while  $\theta < 0$  indicates that it is ‘under pressure’.

### 3. Energy conditions

The four standard energy conditions of GR formulated in terms of the components of the energy-momentum tensor of the gravastar shell — the surface energy density  $\sigma$  (10) and isotropic surface tension  $\theta$  (11) — read as follows

- Weak energy condition (WEC):  $\sigma \geq 0$  and  $\sigma - \theta \geq 0$ ,
- Null energy condition (NEC):  $\sigma - \theta \geq 0$ ,
- Strong energy condition (SEC):  $\sigma - \theta \geq 0$  and  $\sigma - 2\theta \geq 0$ ,
- Dominant energy condition (DEC):  $\sigma \geq 0$  and  $\sigma - |\theta| \geq 0$ .

One can see from the structure of (10) and (11) that the status of the energy conditions for the gravastar shell can be studied in the space of the three configuration variables,  $x, y, z \in [0, 1]$ . As pointed out in Introduction, we require that the energy momentum tensor of the gravastar shell satisfies all energy conditions except the SEC. Since the DEC is more restrictive than the WEC or the NEC, we proceed to consider the DEC through a number of steps.

We begin with the condition of non-negative surface energy density which, as can be easily seen from (10), reduces to

$$\sigma \geq 0 \quad \Longrightarrow \quad x \leq y. \quad (12)$$

This requirement has already been encoded in (6).

Continuing with the condition  $\sigma - |\theta| \geq 0$ , we break it into cases according to  $\theta \lesseqgtr 0$ . We find

$$\theta \lesseqgtr 0 \quad \Longrightarrow \quad x \gtrless f_0(y, z), \quad (13)$$

where the function  $f_0$  is given by

$$f_0(y, z) = \frac{1}{32} \left( 13 + y + 6z - \frac{(1 - 3z)^2}{1 - y} - \frac{2 - y - 3z}{1 - y} \sqrt{36 + y^2 - 6y(6 - z) - 3z(4 - 3z)} \right). \quad (14)$$

The configurations with  $\theta = 0$  (vanishing surface tension/pressure), satisfying  $x = f_0(y, z)$ , are understood as the shells of dust. The DEC is clearly satisfied for dust shells provided (12) holds. For the case  $\theta < 0$ , i.e. shells under (positive) surface pressure, the condition  $\sigma - |\theta| \geq 0$  reduces to

$$\theta < 0, \quad \sigma + \theta \geq 0 \quad \Longrightarrow \quad f_0(y, z) < x \leq f_+(y, z), \quad (15)$$

where  $f_+$  is given by

$$f_+(y, z) = \frac{1}{128} \left( 61 + 25y + 30z - \frac{(1 - 3z)^2}{1 - y} - \frac{6 - 5y - 3z}{1 - y} \sqrt{100 + 25y^2 - 9(4 - z)z - 2y(62 - 15z)} \right). \quad (16)$$

For the case  $\theta > 0$ , i.e. shell under (positive) tension,  $\sigma - |\theta| \geq 0$  reduces to

$$\theta > 0, \quad \sigma - \theta \geq 0 \quad \Longrightarrow \quad f_-(y, z) \leq x < f_0(y, z), \quad (17)$$

where

$$f_-(y, z) = 1 - \frac{4(1 - y)}{(2 - 3y + 3z)^2}. \quad (18)$$

Combining the above cases with the condition (12) allows us to summarize the DEC (which includes the WEC and the NEC) with the following conditions on the configuration variables  $x, y, z \in [0, 1]$ :

$$x \leq y, \quad \begin{cases} f_0(y, z) < x \leq f_+(y, z) & \theta < 0 \quad (\text{pressure}) \\ x = f_0(y, z) & \theta = 0 \quad (\text{dust}) \\ f_-(y, z) \leq x < f_0(y, z) & \theta > 0 \quad (\text{tension}) \end{cases} \quad (19)$$

The configurations saturating the DEC with  $x = f_+$  and  $x = f_-$  can be called stiff and anti-stiff shells. The implications of these conditions on the allowed gravastar configurations are studied in the next Section.

#### 4. Allowed configurations

The shape of the functions  $f_0$ ,  $f_+$  and  $f_-$ , given by (14), (16) and (18), determines the regions in the space of configuration variables  $x, y, z \in [0, 1)$  that are allowed by the DEC (19). In addition, we recall the ‘gravastar condition’  $z \leq x$ , expressing the requirement that the (dark) energy density inside the gravastar is not less than the energy density in the exterior spacetime. Before dividing the analysis into cases corresponding to specific ranges of the configuration variable  $z$ , we observe some general properties of  $f_0$ ,  $f_+$  and  $f_-$ .

As already pointed out in Sec. 2,  $y < z$  implies  $M < 0$  (see Eq. (4)), but it can also be shown that

$$f_-(y, z) > f_+(y, z), \quad 0 \leq y < z < 1, \quad (20)$$

i.e., the DEC (19) cannot be satisfied with  $y < z$ .

For  $y = z$ , which corresponds to  $M = 0$ , one can show that

$$f_-(y, z) = f_0(y, z) = f_+(y, z) = z, \quad 0 \leq z = y < 1, \quad (21)$$

indicating that the only  $y = z$  configuration satisfying the DEC is  $x = y = z$ , which further implies  $\lambda_{\text{int}} = \lambda_{\text{ext}}$ , i.e., simply de Sitter spacetime with no gravastar.

For  $y > z$  it can be shown that the following relations hold,

$$f_0(y, z) < f_+(y, z) < y, \quad 0 < z < y < 1. \quad (22)$$

This indicates that the DEC satisfying configurations with  $\theta < 0$  (shell under surface pressure) exist for all  $z$ .

In Fig. 1 the DEC satisfying gravastar configurations are indicated with the shaded regions in the  $x, y$  plane for several fixed values of  $z$ . Details are discussed in what follows.

##### 4.1. $z = 0$

With  $z = 0$  we are actually considering the gravastar with the Schwarzschild exterior geometry. One can show that  $f_0(y, 0) < 0$  for  $0 < y < 1$ , meaning that in this case the dust shells and the shells under surface tension cannot satisfy the condition (6). Inspection of  $f_+(y, 0)$  reveals that it is greater than zero for  $0 < y < 24/25$  with a maximum at  $y = 4/5$ ,

$$f_+(4/5, 0) = \frac{1}{32}(19 - \sqrt{105}) \simeq 0.274. \quad (23)$$

It follows that the  $z = 0$  gravastar configurations allowed by the DEC involve the shell under surface pressure and are constrained by

$$0 = z \leq y \leq 24/25, \quad 0 \leq x \leq f_+(y, 0). \quad (24)$$

The corresponding region in the  $x, y$  plane is shown in Fig. 1 (upper-left plot).

In the original Mazur–Mottola gravastar model it is assumed that the compactness on both sides of the vacuum phase transition layer will approach unity (horizon formation) to induce the vacuum phase transition, i.e.  $x, y \rightarrow 1$ . As we can see from the above analysis, the DEC satisfying configurations are clearly pushed away from the Mazur–Mottola limit. The highest compactness on the exterior side of the gravastar shell that can be reached without violating the DEC is  $y_{\max} = 24/25$ . It corresponds to the surface gravitational redshift  $Z_{\max} = (1 - y_{\max})^{-1/2} - 1 = 4$ , and is obtained with flat interior geometry. The same upper bound on the surface compactness was obtained in a similar context [21] where the DEC-satisfying shell was considered outside of a Schwarzschild black hole of mass  $m$ , in the limit where  $m \rightarrow 0$ . The finding which is relevant in the context of the gravastar model is that the introduction of the de Sitter geometry (dark energy) in the interior, relative to the flat interior geometry (hollow shell), does not help to support the DEC-satisfying shell against the collapse at high values of the surface compactness, as it might be naively expected due to the repulsive character of the de Sitter interior (free falling particle accelerating away from the centre). We have also obtained the upper bound on the compactness at the interior side of the shell; the highest  $x$  that can be reached without violating the DEC is  $x_{\max} \simeq 0.274$ , given by (23), lowering the maximal exterior compactness to  $y = 4/5$  (surface redshift  $Z = \sqrt{5} - 1 \simeq 1.236$ ). Let us also note that in the model of Mazur and Mottola the vacuum phase transition shell is contributing a negligible fraction to the net gravitational mass of the gravastar. Here we see that such a condition cannot be met if the DEC is to be satisfied.

#### 4.2. $0 < z < 1/3$

With  $z > 0$  we are introducing the Schwarzschild–de Sitter exterior geometry. Let us begin with the configurations with the gravastar shell under (positive) surface pressure ( $\theta < 0$ ). The functions  $f_0$  and  $f_+$  tend to  $-\infty$  as  $y \rightarrow 1$ , but they have a maximum in  $y$  with the value greater than  $z$  for  $z < y < 1$ . The area in the  $x, y$  plane bounded by  $f_0$  and  $f_+$  is the  $\theta < 0$  DEC satisfying region, but we must also observe the ‘gravastar requirement’  $x \geq z$ . Therefore we look for the intersections of  $f_0$  and  $f_+$  with the  $x = z$  line and we find

$$f_0(y_0, z) = z, \quad y_0 = y_0(z) = \frac{z(5 - 9z)}{1 - z} \quad (25)$$

and

$$f_+(y_+, z) = z, \quad y_+ = y_+(z) = \frac{24 - 19z - 9z^2}{25(1 - z)}. \quad (26)$$

The DEC satisfying gravastar configurations with the shell under surface pressure ( $\theta < 0$ ) are therefore

$$0 < z < 1/3, \quad \begin{cases} f_0 < x \leq f_+(y, z) & \text{for } z < y \leq y_0(z) \\ z \leq x \leq f_+(y, z) & \text{for } y_0 < y \leq y_+(z) \end{cases} \quad (27)$$



where  $y_0$  and  $y_+$  are given by (25) and (26). The dust shells ( $\theta = 0$ ) configurations are those with

$$0 < z < 1/3, \quad x = f_0(y, z), \quad z < y \leq y_0. \quad (28)$$

Upon showing that  $f_-(y, z) < z$  for  $z < y < y_0(z)$  it follows that the DEC satisfying configurations with the shell under surface tension ( $\theta > 0$ ) are

$$0 < z < 1/3, \quad z < x < f_0(y, z), \quad z \leq y \leq y_0. \quad (29)$$

The DEC satisfying gravastar configurations for the case  $z = 1/4$  are shown in Fig. 1 (upper-right plot).

Considering  $z > 0$  puts the gravastar model into the context where positive cosmological constant  $\Lambda$  is present in the Einstein equations. Here we can no longer discuss the surface gravitational redshift, but we still find it important to discuss the maximal surface compactness that can be reached without violating the DEC. As in the  $z = 0$  case, the highest compactness on the exterior side of the shell is achieved with the ‘hollow interior’,  $x = z$ , which here means that the (dark) energy density in the interior is equal to that in the exterior; the maximal compactness is  $y_+(z)$  given in (26). It can be shown that  $y_+(z)$  starts with the value  $24/25$  at  $z = 0$  and increases toward unity as  $z \rightarrow 1/3$ . However, if the (dark) energy density in the interior is higher than that in the exterior region,  $x > y$ , the maximal compactness that can be achieved is lower than that given by  $y_+$ . Another interesting feature of gravastar configurations with  $z > 0$  is that in addition to the configurations with shell under surface pressure here we can have shells of dust and shells under surface tension.

### 4.3. $z = 1/3$

The  $z = 1/3$  case can be seen as the critical case between the regimes  $z \leq 1/3$ . The functions  $f_0(y, 1/3)$  and  $f_+(y, 1/3)$ , bounding the  $\theta < 0$  DEC satisfying region, are monotonically increasing in  $y$  for  $1/3 < y < 1$ , reaching finite values  $f_0(1, 1/3) = 1/2$  and  $f_+(1, 1/3) = 3/4$ , while  $f_-(y, 1/3)$  is monotonically decreasing diverging to  $-\infty$  as  $y \rightarrow 1$ . Observing also the ‘gravastar requirement’  $x \geq z$ , the DEC satisfying configurations are simply

$$1/3 = z \leq y < 1, \quad \begin{cases} f_0(y, z) < x \leq f_+(y, z) & (\theta < 0) \\ x = f_0(y, z) & (\theta = 0) \\ z \leq x < f_0(y, z) & (\theta > 0) \end{cases} \quad (30)$$

and are shown in Fig. 1 (lower-left plot). The distinctive feature of this special case  $z = 1/3$  is that there is a wide range of configurations that allow the surface compactness on the exterior side to approach unity arbitrarily close. The compactness on the interior side of the shell is still bounded from above by  $f_+$ , or fixed by  $f_0$  for a dust shell. For example, the dust shell with  $y \rightarrow 1$  will have  $x \rightarrow 1/2$ , which implies interior (dark) energy density which higher by factor  $x/z \rightarrow 3/2$  than the (dark) energy density in the exterior. However, the value of  $z = 1/3$  considered here implies that the radius

of the gravastar is larger than one half of the radius of the exterior horizon of the Schwarzschild–de Sitter geometry, which makes these configurations highly unlikely to be relevant in the astrophysical context.

#### 4.4. $1/3 < z < 1$

For completeness here we consider also the  $1/3 < z < 1$  configurations. The functions  $f_-$ ,  $f_0$  and  $f_+$  tend to 1 as  $y \rightarrow 1$ . Since  $f_0 \geq z$  for  $1/3 < y < 1$ , the configurations with dust shells and shells under surface pressure ( $\theta \leq 0$ ) are

$$1/3 < z < y < 1, \quad f_0(y, z) \leq x \leq f_+(y, z). \quad (31)$$

The shell under tension ( $\theta > 0$ ) configurations must be treated more carefully since it can be shown that the function  $f_-(y, z)$  dips into the  $x < z$  region for  $1/3 < z < 2/3$ , which is forbidden by the ‘gravastar requirement’  $z \leq x$ . We find

$$f_-(y_-, z) = z, \quad y_- = y_-(z) = \frac{8 - 3z - 9z^2}{9(1 - z)}, \quad (32)$$

so for  $1/3 < z < 2/3$ , the  $\theta > 0$  DEC satisfying gravastar configurations are

$$1/3 < z < 2/3, \quad \begin{cases} z < y \leq y_-, & z \leq x < f_0(y, z) \\ y_- < y < 1, & f_-(y, z) \leq x < f_0(y, z) \end{cases} \quad (33)$$

where  $y_-$  is given by (32). For  $2/3 \leq z < 1$  the  $\theta > 0$  DEC satisfying gravastar configurations are

$$2/3 \leq z < y < 1, \quad f_-(y, z) \leq x < f_0(y, z). \quad (34)$$

The special case  $z = 1/2$  is shown in Fig. 1 (lower-right plot). The interesting feature of  $z > 1/3$  configurations is that the compactness on both sides of the shell can approach unity without violating the DEC. However, as already commented in the case of  $z = 1/3$  configurations, the size of such object is too large to represent a body of astrophysical interest.

## 5. A note on the equation of state

In a perfect fluid described by an equation of state of the form  $p = p(\rho)$ , where  $p$  is the isotropic pressure and  $\rho$  is the energy density, the speed of sound propagation,  $c_s$ , is given by the relation  $c_s^2 = dp/d\rho$ . In order for the causality to be preserved, it is natural to require that the sound speed does not exceed the speed of light, i.e. in our units  $c_s < 1$ . For a view on the status of the relation among causality and the speed of sound see Ref. [22]. Here we will investigate the speed of sound propagating (tangentially) along the gravastar shell, assuming that the equation of state for matter comprising the shell can be given in the simple (barotropic) form  $\theta = \theta(\sigma)$ . Note that while the matter comprising the shell can be considered as the perfect fluid on the hypersurface, in the complete spacetime it represents a highly anisotropic structure (the transverse pressure is described by the  $\delta$ -distribution).

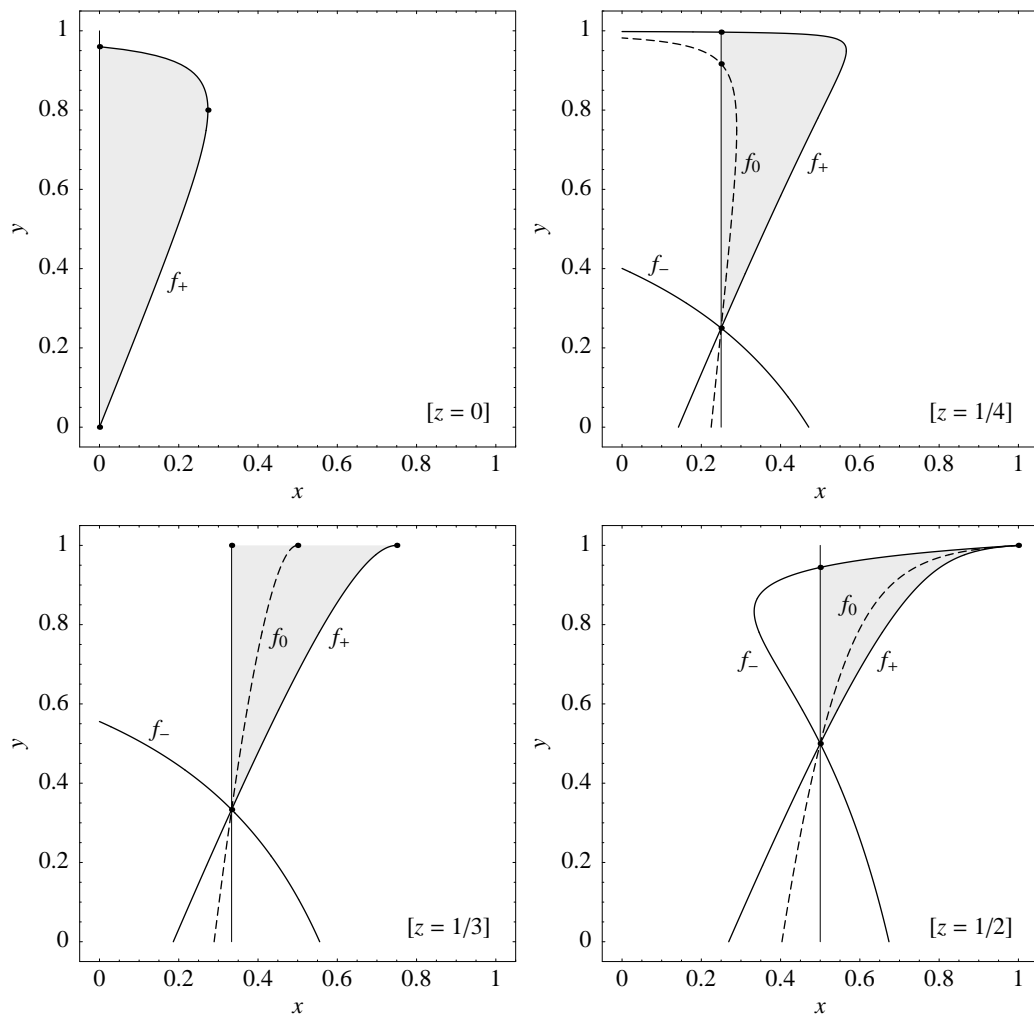


**Figure 1.** Gravastar configurations allowed by the DEC shown as shaded regions in the  $x, y$  plane for fixed values of  $z = 0, 1/4, 1/3, 1/2$ . ( $x, y, z$  are defined in (5))

In Ref. [3] a procedure has been developed that allows extracting of the equation of state  $\theta = \theta(\sigma)$  of the matter comprising the gravastar shell on the basis of the requirement that the shell be stable against radial perturbations. From the dynamical version of the expressions for the surface energy density and the surface tension of the shell, which involve the terms  $\dot{a}^2$  and  $\ddot{a}$ , overdot indicating the derivative with respect to the proper time of the observer co-moving with the shell, the ‘classical’ equation of motion of the form  $\frac{1}{2}\dot{a}^2 + V = E$  follows. The ‘potential’  $V$  is a function of the gravastar radius  $a$  and other configuration variables, while the ‘energy’  $E \equiv 0$  (one is not allowed to adjust the energy as in the classical context). Upon identifying  $\dot{a}^2 = -2V(a)$  and  $\ddot{a} = -V'(a)$  (See Ref. [3] for the full derivation) the dynamical expressions for  $\sigma$  and  $\theta$  become functions of the dynamical gravastar radius. The requirement for the stability of a shell at the radius  $a$  can then be expressed as the requirement imposed on the potential,

$$V(a) = 0, \quad V'(a) = 0, \quad V''(a) \geq 0. \quad (35)$$

Therefore, if one chooses a particular shape of the potential  $V(a)$  leading to stable gravastar shells, the equation of state  $\theta = \theta(\sigma)$  can be parametrically extracted by varying  $a$  over the range of interest. The important special case is  $V(a) \equiv 0$  which, as argued in Ref. [3], reflects the notion of strict stability of the shell. If the shell would be displaced to a nearby radius, it would find itself there in a new state of equilibrium. In the case  $V(a) \equiv 0$  the dynamical equations for surface energy density and surface pressure of the shell coincide with (reduce back to) the static expressions for  $\sigma$  and  $\theta$  given by (10) and (11). Therefore we can use this approach to compute the quantity

$$c_s^2 = -\frac{d\theta}{d\sigma} = -\frac{d\theta/da}{d\sigma/da} \quad (36)$$

directly from (10) and (11).

We now proceed to compute  $c_s^2$  for the gravastar models we have considered so far. Using (36), (10) and (11) one can obtain an expression for  $c_s^2$  in terms of  $a$ ,  $\lambda_{\text{int}}$ ,  $\lambda_{\text{ext}}$  and  $M$  which is rather involved, but with the use of our configuration variables  $x, y, z$  defined in (5) it becomes much more compact and can be written

$$c_s^2 = \frac{4v^3 - u^3[1 - 6z + 3(v^2 + z)(v^2 + 3z)]}{4u^2v^2[-2v + u(-1 + 3v^2 + 3z)]} \quad (37)$$

where  $u^2 = 1 - x$  and  $v^2 = 1 - y$ . The quantity  $c_s^2$  diverges for  $u \rightarrow 0$  and  $v \rightarrow 0$  and also at  $u = 2v/(3v^2 + 3z - 1)$ . To obtain the boundaries of the regions in the  $x, y$  plane (for the given values of  $z$ ) in which  $0 \leq c_s^2 \leq 1$  one must solve  $c_s^2 = 0, 1$  for  $u$  which leads to a cubic equation. The resulting expressions are very complicated so we only plot the results for  $z = 0$  (Schwarzschild exterior geometry) and  $z = 1/3$  (case considered in Sec. 4.3) in Fig. 2. The region where causality is preserved with the equation of state having usual properties (surface pressure increases as energy density increases) are indicated by ‘A’. We can see that the causality requirement combined with the energy conditions considered before imposes still stronger upper bounds on the gravastar exterior surface compactness  $y$ . As an example, for the  $x = z = 0$  case (hollow shell, Schwarzschild exterior) the highest allowed surface compactness is  $y_{\text{max}} \simeq 0.848$  or analytically  $2(106 + \alpha - 89/\alpha)/255$  where  $\alpha = (225\sqrt{106} - 2195)^{1/3}$ . In both examples shown in Fig. 2 we also see that the region ‘C’ where  $c_s^2$  is negative includes some regions that are allowed by the energy conditions. Negative  $c_s^2$  means that the surface pressure decreases as the surface energy density increases, which indicates instability with respect to perturbations. Therefore, the requirement that the dependence of  $\theta$  on  $\sigma$  is such that stability with respect to radial perturbations is obtained can lead to configurations where the gravastar shell is unstable against tangential perturbations such as sound propagation.

## 6. Conclusions

Compact objects like gravastars envisaged as possible alternatives to black holes are certainly not less controversial than black holes themselves [23]. The essential

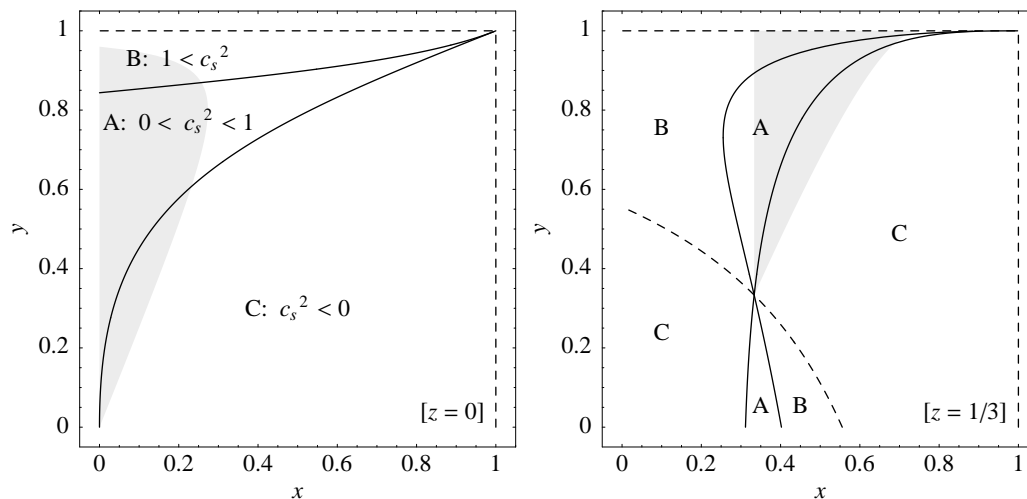


**Figure 2.** Behaviour of the quantity  $c_s^2 = -d\theta/d\sigma$  (speed of sound squared) as derived from the requirement for the stability against the radial perturbations for the gravastar shells with  $z = 0$  (left plot) and  $z = 1/3$  (right plot), shown in the  $x, y$  plane. Dashed lines indicate configurations where  $c_s^2 \rightarrow \pm\infty$ , while the solid lines bound the region ‘A’ in which  $0 < c_s^2 < 1$ . Region ‘B’ is the  $1 < c_s^2$  superluminal regime, while ‘C’ is the  $c_s^2 < 0$  unstable regime. Shaded regions are the gravastar configurations allowed by the DEC (See Fig. 1).

phenomenological feature of a gravastar that makes it difficult to distinguish such a body from a true black hole is its high surface redshift. Also, the analysis of radiation from a supermassive object Sgr A\* [24] implied the existence of a horizon in this object. However, the absence of detectable heating could also be consistent with a gravastar possessing sufficiently large heat capacity [10]. Another feature which may help in this respect is the analysis of quasi-normal modes of oscillation of a gravastar. They are found to be different from those of a black hole [9], and could, in principle, provide a way to observationally discern a gravastar from a black hole. In the same spirit it is important to analyze the constraints on possible realisations of gravastar models. Since the physical theory behind the quantum vacuum phase transitions which are assumed to take place within the gravastar shell has not been fully formulated, the energy conditions of GR provide the most general model-independent constraint on the structure of the energy-momentum tensor of the gravastar. We have carried out a detailed analysis of the constraints that the energy conditions impose on the possible configurations of the single  $\delta$ -shell version of the gravastar model [3].

The most relevant constraint is the upper bound on the surface compactness  $\mu = 2m/r$  of the gravastar which was in the original MM model assumed to approach unity arbitrarily close. Exactly this feature gives rise to arbitrarily large surface gravitational redshift which makes the gravastar observationally difficult to distinguish from the true Schwarzschild black hole. (Note that the original MM model violates the DEC at its two  $\delta$ -shells that are assumed to possess nonvanishing surface pressure but vanishing surface energy density. For a general discussion of known violations of energy

conditions see eg. Refs [19, 25]).

In this paper we have derived the bounds on the surface compactness that follow from the requirement that the matter comprising the gravastar shell satisfies the DEC. The procedure is fully analytic and has been made possible by the use of the configuration variables  $x, y, z$  based the values of the compactness at the inner and the outer side of the shell defined in (5). The space of gravastar configurations satisfying the DEC is confined within the range  $f_-(y, z) \leq x \leq f_+(y, z)$ , where the functions  $f_-$  and  $f_+$  identifying the configurations with anti-stiff and stiff shells are given by (18) and (16). In case of the Schwarzschild exterior geometry the maximal surface compactness  $\mu_{\max} = y_{\max} = 24/25$  is achieved with a stiff shell and flat geometry in the gravastar interior (compactness in the interior side of the shell  $x = 0$ ), i.e. in the limit of vanishing (dark) energy density in the interior. Introducing the (dark) energy density in the interior ( $x > 0$ ) does not lead to higher surface compactness that can be reached. This finding may be seen as counter-intuitive since one might have expected that the repulsive character of the de Sitter geometry will help to support the shell against the collapse. However, as our analysis has shown, this is not the case if the shell is to satisfy the DEC.

For completeness, we have extended our analysis to the case of the Schwarzschild–de Sitter exterior geometry which places the gravastar model in the context where the positive cosmological constant  $\Lambda$  is present in the Einstein equations. Relevant bounds on the surface compactness have been obtained for all values of the configuration variable  $z = \Lambda a^2/3$ ,  $a$  being the gravastar radius. For  $z < 1/3$  the highest surface compactness is bounded below unity and is achieved with the stiff shell. At  $z = 1/3$  there is a wide range of configurations where the surface compactness can approach unity arbitrarily close and it includes shells under surface pressure, dust shells and shells under surface tension. For  $z > 1/3$  the highest surface compactness is again bounded below unity and is achieved with anti-stiff shells.

We have also applied the procedure of Ref. [3] to compute the quantity  $c_s^2 = -d\theta/d\sigma$  which in the context of perfect fluids corresponds to the speed of sound. In order not to violate the principle of causality one normally requires that the sound speed does not exceed the speed of light. This requirement has given still stronger upper bounds on the gravastar surface compactness as compared to the bounds derived from the energy conditions. However, we must emphasize that the procedure is based on the assumption that the exotic matter comprising the gravastar shell obeys a barotropic equation of state of the form  $\theta = \theta(\sigma)$ , on the assumption that the shell is stable against the radial perturbations, and most importantly on the assumption that the fluctuations in surface tension and surface energy density propagate along the shell at the speed given by the usual formula stated above. Since the full theory describing the gravastar shell is not available none of these assumptions can be taken for granted. Similar situation has been encountered in the context of the stability analysis of wormhole solutions in Ref. [26].

All the above results were derived using the  $\delta$ -shell gravastar model, but they may be relevant in the broader context of the dark energy stars, or gravastars with continuous pressure profiles, where one attempts to construct astrophysically plausible models of

self-gravitating objects with dark-energy cores. As shown in Ref. [7], and applied in Ref. [8], such objects require anisotropic principal pressures. The analysis of the maximal surface compactness of anisotropic spheres is considerably more complicated than in the isotropic case; probably the most general results obtained in this area is Ref. [27], although still not general enough to include the case of the dark energy interior, or Ref. [28] where the influence of the cosmological constant on the compactness and other physical parameters of anisotropic configurations was considered. However, thin shells (soap bubbles) appear to be the most efficient configurations in attempts to reach high surface compactness of anisotropic spherical bodies. The maximal compactness of the ‘shell around a black hole’ of Ref. [21], or that of our flat interior gravastar (hollow shell), clearly saturates the general bound derived in Ref. [27], and similar suggestions have also been given in Ref. [29].

## Acknowledgments

We acknowledge the support from the Croatian Ministry of Science under the project 036-0982930-3144. SI thanks for hospitality the University of Vienna where part of this work was carried out.

## References

- [1] Mazur P O and Mottola E 2001 (*Preprint gr-qc/0109035*)
- [2] Mazur P O and Mottola E 2004 *Proc. Nat. Acad. Sci.* **111** 9545 (*Preprint gr-qc/0407075*)
- [3] Visser M and Wiltshire D L 2004 *Class. Quantum Grav.* **21** 1135 (*Preprint gr-qc/0310107*)
- [4] Carter B M N 2005 *Class. Quantum Grav.* **22** 4551 (*Preprint gr-qc/0509087*)
- [5] Bilić N, Tupper G B and Viollier R D 2006 *J. Cosmol. Astropart. Phys.* **0602** 013 (*Preprint astro-ph/0503427*)
- [6] Lobo F S N and Arellano A V B 2007 *Class. Quantum Grav.* **24** 1069 (*Preprint gr-qc/0611083*)
- [7] Cattoen C, Faber T and Visser M 2005 *Class. Quantum Grav.* **22** 4189 (*Preprint gr-qc/0505137*)
- [8] DeBenedictis A, Horvat D, Ilijić S, Kloster S and Viswanathan K S 2006 *Class. Quantum Grav.* **23** 2303 (*Preprint gr-qc/0511097*)
- [9] Chirenti C B M H and Rezzolla L 2007 (*Preprint 0706.1513[gr-qc]*)
- [10] Broderick A E and Narayan R 2007 *Class. Quantum Grav.* **24** 659 (*Preprint gr-qc/0701154*)
- [11] Lobo F S N 2006 *Class. Quantum Grav.* **23** 1525 (*Preprint gr-qc/0508115*)
- [12] Sakharov A D 1966 *Sov. Phys. JETP* **22** 241
- [13] Gliner E B 1966 *Sov. Phys. JETP* **22** 378
- [14] Dymnikova I 1992 *Gen. Rel. Grav.* **24** 235
- [15] Dymnikova I 2002 *Class. Quantum Grav.* **19** 725 (*Preprint gr-qc/0112052*)
- [16] Dymnikova I and Galaktionov E 2007 *Phys. Lett. B* **645** 358
- [17] Hawking S W and Ellis G F R 1973 *The large scale structure of space-time* (London: Cambridge University Press, Cambridge Monographs on Mathematical Physics)
- [18] Israel W 1966 *Nuovo Cimento B* **44** 1
- [19] Visser M 1996 *Lorentzian Wormholes: From Einstein to Hawking* (AIP Press)
- [20] Poisson E 2004 *A Relativist’s Toolkit: The Mathematics of Black-Hole Mechanics* (Cambridge University Press)
- [21] Frauendiener J, Hoenselaers C and Konrad W 1990 *Class. Quantum Grav.* **7** 585–587
- [22] Ellis G F R, Maartens R and MacCallum M A H 2007 (*Preprint gr-qc/0703121*)

- [23] Lasota J P 2007 *C. R. Physique* **8** 45 (*Preprint astro-ph/0607453*)
- [24] Broderick A E and Narayan R 2006 *Astrophys. J.* **638** L21 (*Preprint astro-ph/0512211*)
- [25] Barcelo C and Visser M 2002 *Int. J. Mod. Phys. D* **11** 1553 (*Preprint gr-qc/0205066*)
- [26] Poisson E and Visser M 1995 *Phys. Rev. D* **52** 7318 (*Preprint gr-qc/9506083*)
- [27] Andreasson H 2007 (*Preprint gr-qc/0702137*)
- [28] Boehmer C G and Harko T 2006 *Class. Quantum Grav.* **23** 6479 (*Preprint gr-qc/0609061*)
- [29] Bondi H 1999 *Mon. Not. R. Astron. Soc.* **302** 337